[redacted]AL

Copy 32
RM SL55I15

CASE FILE
COPY

NACA

RESEARCH MEMORANDUM

for the

Bureau of Aeronautics, Department of the Navy

EFFECTS OF VARIOUS MODIFICATIONS ON THE STATIC LONGITUDINAL STABILITY AND CONTROL CHARACTERISTICS OF A 0.065-SCALE MODEL OF THE CHANCE VOUGHT REGULUS II MISSILE AT A MACH NUMBER OF 2.01

TED NO. NACA AD 398

By Ross B. Robinson and Cornelius Driver

Langley Aeronautical Laboratory
Langley Field, Va.

Declassified by authority of NASA Classification Change Notices No. [illegible]
Dated ** [illegible]

[redacted]DOCUMENT

This document contains classi[redacted]States within the meaning of the Espionage A[redacted] and 794. Its transmission o[redacted]ny manner to an unauth[redacted]rohibited by law.

NATIONAL ADVISORY COMMITTEE
FOR AERONAUTICS

WASHINGTON

SEP 26 1955

[redacted]

DECLASSIFIED

NATIONAL ADVISORY COMMITTEE FOR AERONAUTICS

RESEARCH MEMORANDUM

for the

Bureau of Aeronautics, Department of the Navy

EFFECTS OF VARIOUS MODIFICATIONS ON THE STATIC LONGITUDINAL STABILITY AND CONTROL CHARACTERISTICS OF A 0.065-SCALE MODEL OF THE CHANCE VOUGHT REGULUS II MISSILE AT A MACH NUMBER OF 2.01

TED NO. NACA AD 398

By Ross B. Robinson and Cornelius Driver

SUMMARY

An investigation has been conducted in the Langley 4- by 4-foot supersonic pressure tunnel to determine the effects on the static longitudinal stability and control characteristics of various modifications to a 0.065-scale model of the Chance Vought Regulus II missile. The modifications consisted of a control housing on top of the fuselage, two sizes of canard surfaces with fixed incidence angles, various angles of nose droop, and two types of inlet boundary-layer bleed diverters. The tests were made at a Mach number of 2.01 and a Reynolds number, based on the mean aerodynamic chord of 1.54×10^6.

INTRODUCTION

One of the most significant results of a previous investigation of the Regulus II missile at Mach numbers of 1.41 to 2.01 (ref. 1) was the large negative value of pitching-moment coefficient at zero lift (C_{m_o}) for zero control deflection. A free-flight rocket model test (unpublished) showed the same result, the value of the negative C_{m_o} obtained being somewhat larger than that for the tunnel model. The occurrence of these

large values of C_{m_o} necessitates large control deflections for trim with a resultant increase in drag and loss of maneuverability.

The results presented in reference 1 indicate that the negative increments of C_{m_o} might be attributable, in part, to effects of the underslung scoop-type inlet. In addition, static loadings of the free-flight model produced moderate deflections of a long section of the nose. Since both the free-flight model and a production missile would be more flexible than the wind-tunnel model, additional negative increments in C_{m_o} might be expected.

Means of reducing this initial negative C_{m_o} are of considerable importance. The basic tunnel model previously tested was modified to provide experimental information on the use of canard surfaces to produce a positive increment in C_{m_o} for zero control deflection and on the effects of nose droop on the longitudinal characteristics. Other modifications to the configuration included an external control housing on top of the fuselage and means for varying the amount of flow through the boundary-layer bleed of the scoop-type inlet.

This report presents the results of an investigation of the effects of these modifications on the aerodynamic characteristics in pitch of the Regulus II missile at $M = 2.01$ in the Langley 4- by 4-foot supersonic pressure tunnel.

COEFFICIENTS AND SYMBOLS

The results of the tests are presented as standard NACA coefficients of forces and moments. The data are referred to the stability-axes system (fig. 1) with the reference center of moments on the longitudinal center line of the basic body of revolution at a longitudinal station corresponding to the leading edge of the wing mean geometric chord (fig. 2).

The coefficients and symbols are defined as follows:

C_L	lift coefficient, $-Z/qS$
C_D	drag coefficient, Drag/qS
C_m	pitching-moment coefficient, $M'/qS\bar{c}$
C_{m_o}	pitching-moment coefficient at $C_L = 0$
X	force along X-axis

Z	force along Z-axis
M'	moment about Y-axis
q	free-stream dynamic pressure
M	Mach number
S	wing area including body intercept, 88.47 sq in.
S_c	exposed area of canard surface
$\frac{S_c}{S_w}$	ratio of exposed area of canard to total wing area
b	wing span, 15.63 in.
c	chord, in.
$\bar{c}$	wing mean geometric chord, 5.78 in.
α	angle of attack of fuselage center line, deg
t	airfoil thickness, in.
x	chordwise distance from leading edge of airfoil section, in.
δ_c	canard deflection with respect to fuselage center line, deg
δ_e	elevon deflection normal to hinge line, deg
L/D	lift-drag ratio, C_L/C_D
m/m_o	mass-flow ratio

Subscripts:

trim	measured for $C_m = 0$
R	right
L	left

[redacted]

MODEL AND APPARATUS

A three-view drawing of the basic model and details of various components are presented in figures 2 and 3. Details of the various modifications are shown in figure 4. The geometric characteristics of the model are presented in table I.

The model was equipped with a wing having 43.5° of sweep of the quarter-chord line, aspect ratio 2.75, taper ratio 0.6, and modified circular-arc airfoil sections of 4-percent thickness-chord ratio. (See table I.) The wing was mounted 0.26 inch above the fuselage center line and had zero incidence and dihedral.

Elevons of the plain trailing-edge-flap type provided both longitudinal and lateral control (fig. 2). The model had a swept vertical tail and movable rudder (fig. 2). Deflections of all control surfaces were set manually. The rudder deflection was 0° for the entire test.

Coordinates of the basic fuselage are presented in table II. A simulated static pressure probe was attached to the nose of the fuselage. A scoop inlet equipped with a boundary-layer diverter (fig. 3) was incorporated into the fuselage to simulate the internal flow conditions of the missile. The inlet airflow, which could be throttled manually to provide variable mass-flow ratios, was discharged out the rear of the fuselage around the sting. A solid fairing (fig. 3) was used to permit investigations of the model with no internal airflow ("inlet faired closed" configuration).

Modifications to the basic model (fig. 4) consisted of: (a) a control housing on the top of the fuselage; (b) two fixed-incidence horizontal canard surfaces, the larger having a 9.5° incidence angle, the smaller having a 19.1° incidence angle; (c) various wedges to provide nose-droop angles of 0°, -1.65°, and -3.00°; and (d) inlet boundary-layer bleed diverters to provide 40-percent and 100-percent closure of the original bleed. When the boundary-layer bleed was completely closed, the bleed outlet under the wing was also sealed.

Force and moment measurements were made through the use of an experimental, all welded, six-component strain-gage balance furnished by the NACA. This experimental balance is characterized by an extremely small size but has an attendant increase in balance deflections and interactions. Space limitation was the primary consideration in its selection.

The following pressure measurements were made:

(1) the static pressure in the balance chamber inside the model, (2) the static pressure on the rim base area of the fuselage, and (3) the

DECLASSIFIED

total and static pressures of the exit airflow with open inlet by means of a total head rake fastened to the sting at the base of the model.

TEST CONDITIONS AND PROCEDURE

The conditions for the tests were:

Mach number	2.01
Reynolds number, based on $\bar{c}$	1.54×10^6
Stagnation pressure, lb/sq in.	13
Stagnation temperature, $^{\circ}F$	100
Stagnation dewpoint, $^{\circ}F$	<-25
Mach number variation	± 0.015
Flow angle in horizontal or vertical plane, deg	± 0.1

Tests were made through an angle-of-attack range from about -4° to about $+12^{\circ}$ at zero angle of sideslip.

CORRECTIONS AND ACCURACY

The angles of attack and sideslip were corrected for the deflection of the balance and sting under load. The nominal values for elevon deflection presented in this report are not corrected for deflection due to load. Although the variation of rudder deflection was not known, it was assumed to be small (within $\pm 0.1^{\circ}$) since the surface was rigidly fixed in the desired position by a bead of solder along the leading edge of the rudder.

Base pressure measurements were made and the longitudinal-force coefficients of all configurations were adjusted to free-stream static pressure at the base. For all configurations with the open inlet, the internal pressure in the model balance chamber was measured and corrections for a buoyant force on the balance were applied to the results. The internal drag was determined from the change in momentum from free-stream conditions to measured conditions at the duct exit. Base drag, buoyant force, and internal drag have been subtracted from the total longitudinal-force measurements so that a net external longitudinal-force coefficient was obtained. The mass-flow ratio was 0.93. The magnitude of the base, internal, and buoyant drag coefficients at $\alpha = 0^{\circ}$ is indicated by the following table:

Base C_D	-0.0001
Internal C_D	0.0050
Buoyant C_D	-0.0125

[redacted]

The estimated errors in the individual measured quantities are as follows:

C_L	±0.003
C_D	±0.002
C_m	±0.005
α, deg	±0.1
δ_e (corrected for deflection of elevon under load), deg	±0.1
M	±0.015

RESULTS AND DISCUSSION

Effects of Nose Droop

Negative deflection of the nose produced a progressive negative shift of pitching-moment coefficient (fig. 5). It is possible that nose bending contributed to the more negative C_{m_o} experienced by the free-flight rocket model (unpublished results). The results of the present wind-tunnel tests indicate that a nose droop of about 2^o would be required to produce the free-flight C_{m_o} value.

It might be expected that positive deflection of the nose could profitably be used to produce a positive C_{m_o} shift and thereby reduce the control deflection required for trim.

There was no appreciable effect of nose droop on the static stability and no effect on the lift or drag except above $C_L \approx 0.3$ where nose droop caused a decrease in C_{L_α} and increased C_D for constant C_L.

Effects of Canards

Addition of either the large or small canards essentially eliminated the large negative value of C_{m_o} (fig. 6); consequently, the elevon deflections required for trim would be reduced. The large positive increment of C_m provided by the larger canard at higher values of C_L probably results from a greater portion of the body nose being affected by the carry-over lift from the canard. The more linear lift and pitching-moment coefficient variation above $C_L \approx 0.4$ for the configurations having the canards may result from downwash from the canards reducing the effective angle of attack of the inboard portion of the wing.

The effects of elevon deflection on the aerodynamic characteristics in pitch for the model with the large canard are shown in figure 7. The effects of the large canard on the longitudinal characteristics for $\alpha = 0^\circ$ and for trim ($C_m = 0^\circ$) are presented in figures 8 and 9, respectively. Results for the basic configuration were obtained from reference 1. At $\alpha = 0^\circ$ the canard produced a slight decrease in total lift coefficient and a positive increment in pitching-moment coefficient, which largely eliminated the negative value of C_{m_o} of the basic configuration (fig. 8). As a result, about 10° less elevon deflection is required to trim the model at zero lift (fig. 9). In addition, the maximum value of $C_{L_{trim}}$ obtainable with an elevon deflection of -20° is increased and the trim drag coefficient is reduced considerably so that higher trim lift-drag ratios are indicated.

Effects of Closure of Inlet Boundary-Layer Bleed

The effects on the longitudinal characteristics of closing the boundary-layer bleed of the open-inlet configuration for zero elevon deflection ($\delta_e = 0$) are shown in figure 10. Reducing the bleed air flow 40 percent had only negligible effects, but completely closing the bleed produced a slightly higher lift-curve slope and a positive shift of the pitching-moment curve, reducing the negative value of C_{m_o} to half that obtained for the open bleed. Similar effects were obtained for $\delta_e = 20^\circ$ with the 100-percent closed bleed (fig. 11). The elevon effectiveness was about the same for the open and fully closed bleed (fig. 11).

Large longitudinal effects were found when the complete inlet was faired closed. The more linear lift curve and the large positive increment in C_m for the faired-closed inlet configuration probably result from the altered pressure distribution on the underside of the wing and the aft portion of the fuselage. Fairing the inlet in this manner produces the effect of a cambered surface with a resulting down load behind the center of moments.

Effects of Control Housing

The addition of the control housing had little effect on the longitudinal characteristics except for a slight negative shift of the pitching-moment curve (fig. 12).

CONCLUSIONS

The results of an investigation of the effects of various modifications to a 0.065-scale model of the Chance Vought Regulus II missile indicate the following conclusions:

1. Negative deflection of the nose produces a progressive negative shift of the pitching-moment curves. It appears possible that nose bending contributed to the more negative value of pitching-moment coefficient for zero lift (C_{m_o}) experienced by a free-flight rocket model.

2. The addition of a fixed-incidence horizontal canard surface resulted in a positive shift in C_{m_o} and a large increase in the trim lift coefficient and the trim lift-drag ratio obtainable.

3. Complete closure of the inlet boundary-layer air bleed resulted in a positive increment of pitching-moment coefficient throughout the lift-coefficient range.

4. Addition of the control housing had negligible effect on the longitudinal characteristics.

Langley Aeronautical Laboratory,
National Advisory Committee for Aeronautics,
Langley Field, Va., August 31, 1955.

Ross B. Robinson
Aeronautical Research Scientist

Cornelius Driver
Aeronautical Research Scientist

Approved:
John V. Becker
Chief of Compressibility Research Division

mjg

REFERENCE

1. Robinson, Ross B., Driver, Cornelius, and Spearman, M. Leroy: Static Longitudinal and Lateral Stability and Control Characteristics of an 0.065-Scale Model of the Chance Vought Regulus II Missile at Mach Numbers of 1.41, 1.61, and 2.01 – TED NO. NACA AD 398. NACA RM SL55E31, Bur. Aero., 1955.

[redacted]

TABLE I

GEOMETRIC CHARACTERISTICS OF MODEL

Wing:	
Total area, including fuselage intercept, sq in.	88.47
Span, in.	15.63
Root chord, in.	7.08
Tip chord, in.	4.27
Length of mean geometric chord, $\bar{c}$, in.	5.78
Aspect ratio	2.75
Taper ratio	0.60
Sweep angle of $\bar{c}/4$ line, deg	43.5
Airfoil section, streamwise –	
Maximum thickness, percent chord	4.0
Location of maximum thickness, percent chord	53.7
Trailing-edge thickness, percent chord	0.04
Symmetric airfoil section defined by $t/c = 0.122496 - 0.015168x/c - (0.028768(x/c)^2 - 0.033096(x/c) + 0.0150052)^{1/2}$	
Dihedral, deg	0
Incidence, deg	0
Elevons:	
Area behind hinge line, each, sq in.	4.61
Moment of area, each, $in.^3$	2.49
Span, in.	3.43
Sweep of hinge line, deg	37.3
Vertical Tail:	
Span (to model center line), in.	5.07
Area (to model center line), sq in.	23.08
Tip chord (theoretical), in.	2.35
Root chord, in.	7.16
Length of tail mean geometric chord, in.	5.28
Aspect ratio	1.12
Taper ratio (theoretical tip)	0.33
Rudder area, sq in.	2.35
Airfoil section	Same as wing

TABLE I.- Concluded

GEOMETRIC CHARACTERISTICS OF MODEL

Fuselage:	
Length (without probe), in.	44.15
Maximum diameter, in.	3.25
Maximum cross-sectional area, sq in.	11.10
Base inner diameter, in.	2.01
Sting diameter, in.	1.25
Area of rim of base, sq in.	0.45
Annular area at base for internal flow, sq in.	1.94
Maximum length-diameter ratio	13.6
Total base area (annular + rim + sting), sq in.	3.62
Canards:	
Small –	
Area (exposed), sq in.	0.64
Span (body included), in.	1.65
Deflection angle, deg	19.1
$\frac{S_c}{S_w}$	0.0072
Large –	
Area (exposed), sq in.	1.28
Span (body included), in.	2.17
Deflection angle, deg	9.5
$\frac{S_c}{S_w}$	0.0144
Dorsal Fairing:	
Length, in.	31.0
Width, maximum, in.	1.4

TABLE II

COORDINATES OF THE BASE FUSELAGE

[x is distance from nose in inches;
r is radius in inches]

x	r
0.000	0.000
.038	.018
.075	.033
.150	.061
.225	.085
.300	.107
.450	.148
.601	.184
.751	.218
.901	.250
1.502	.362
2.252	.486
3.003	.596
3.754	.698
4.505	.792
6.006	.964
7.508	1.117
9.009	1.255
10.511	1.376
12.012	1.478
13.514	1.567
15.015	1.625
34.761	1.625
37.765	1.586
40.086	1.493
41.850	1.345
42.850	1.245
43.850	1.115
44.150	1.065

Figure 1.- System of stability axes. Arrows indicate positive values.

SLRT 2

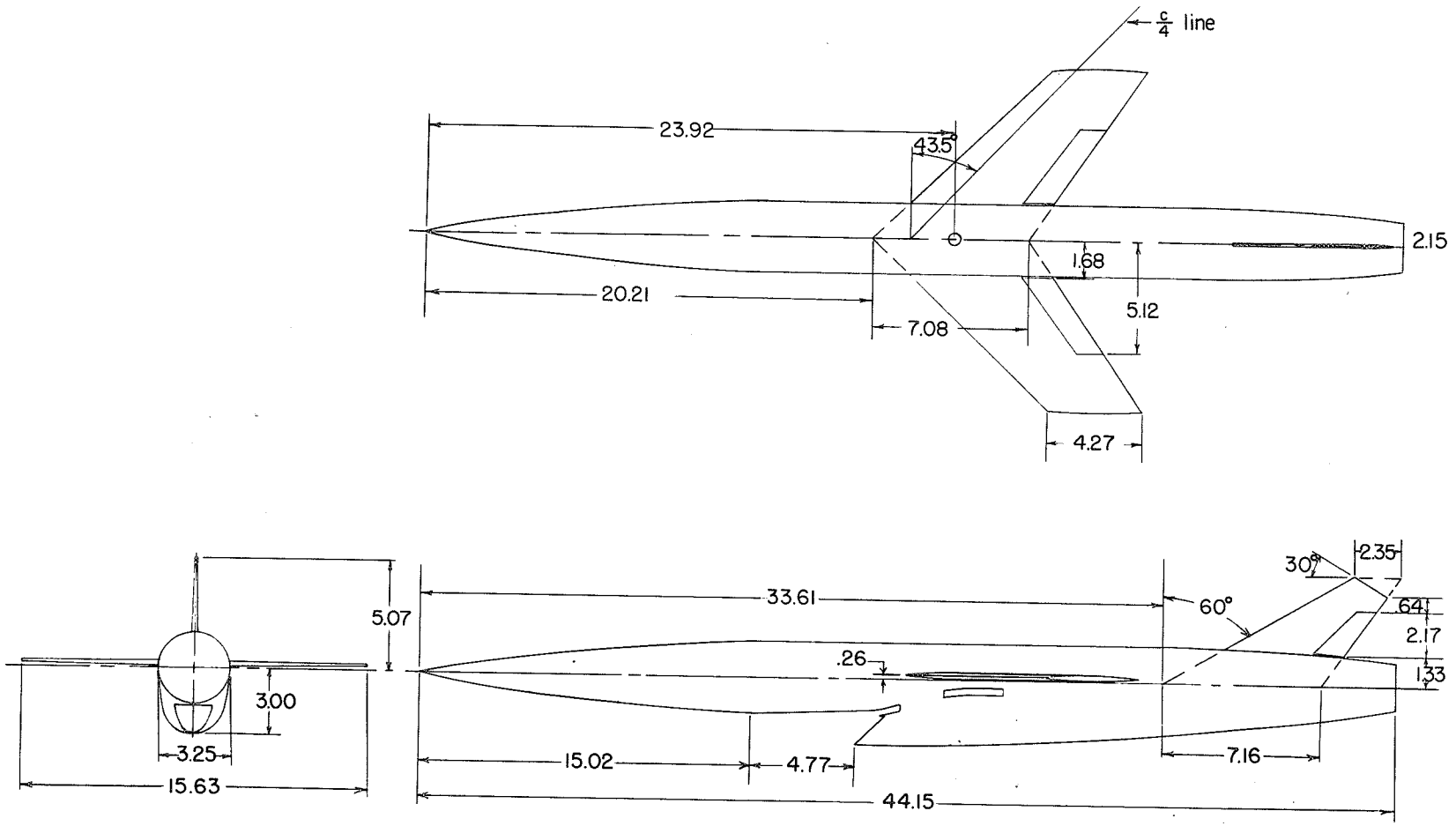

(a) Three-view drawing of model.

Figure 2.- Details of model.

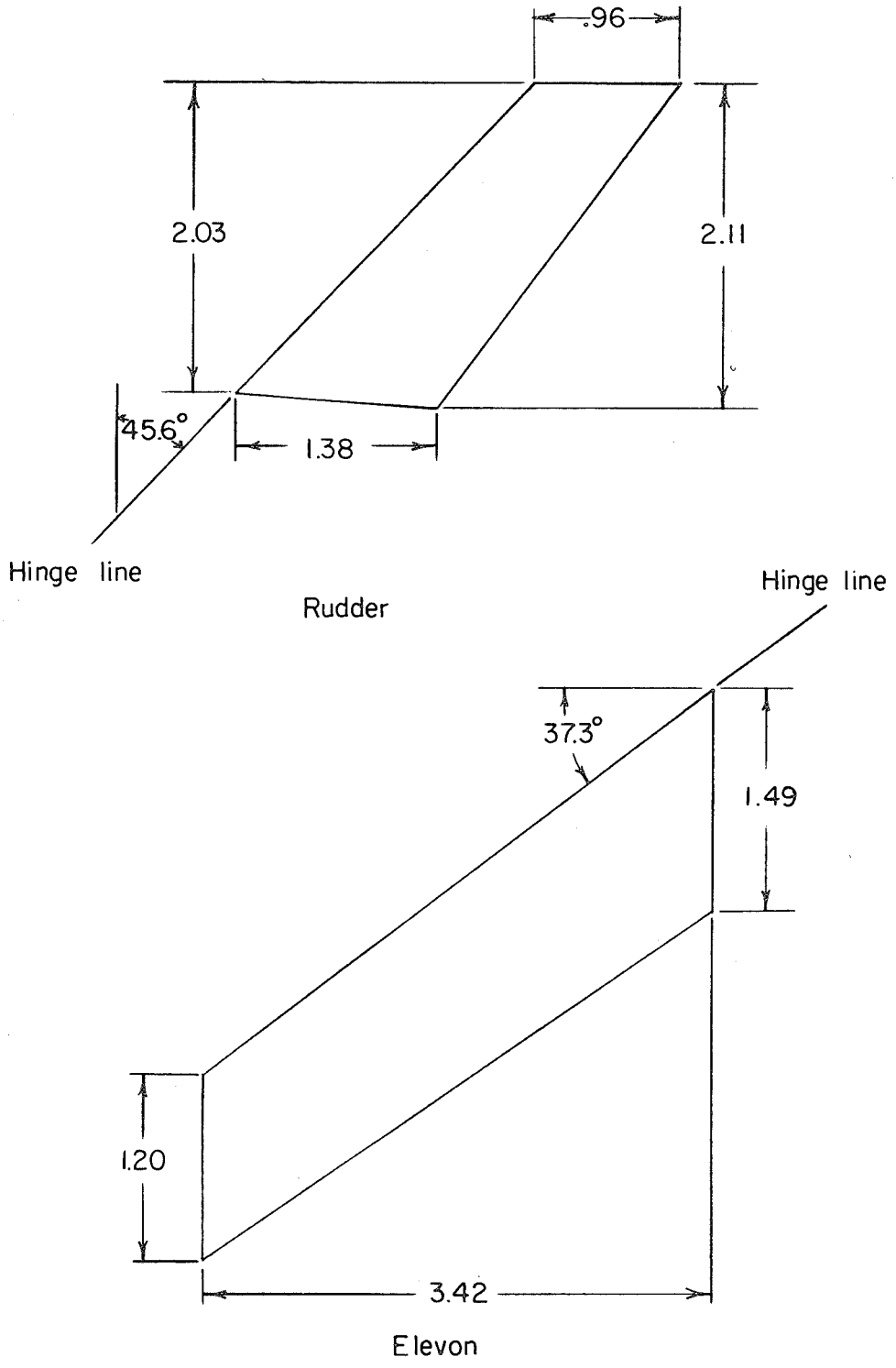

(b) Details of rudder and elevon.

Figure 2.- Concluded.

SECRET

CONFIDENTIAL

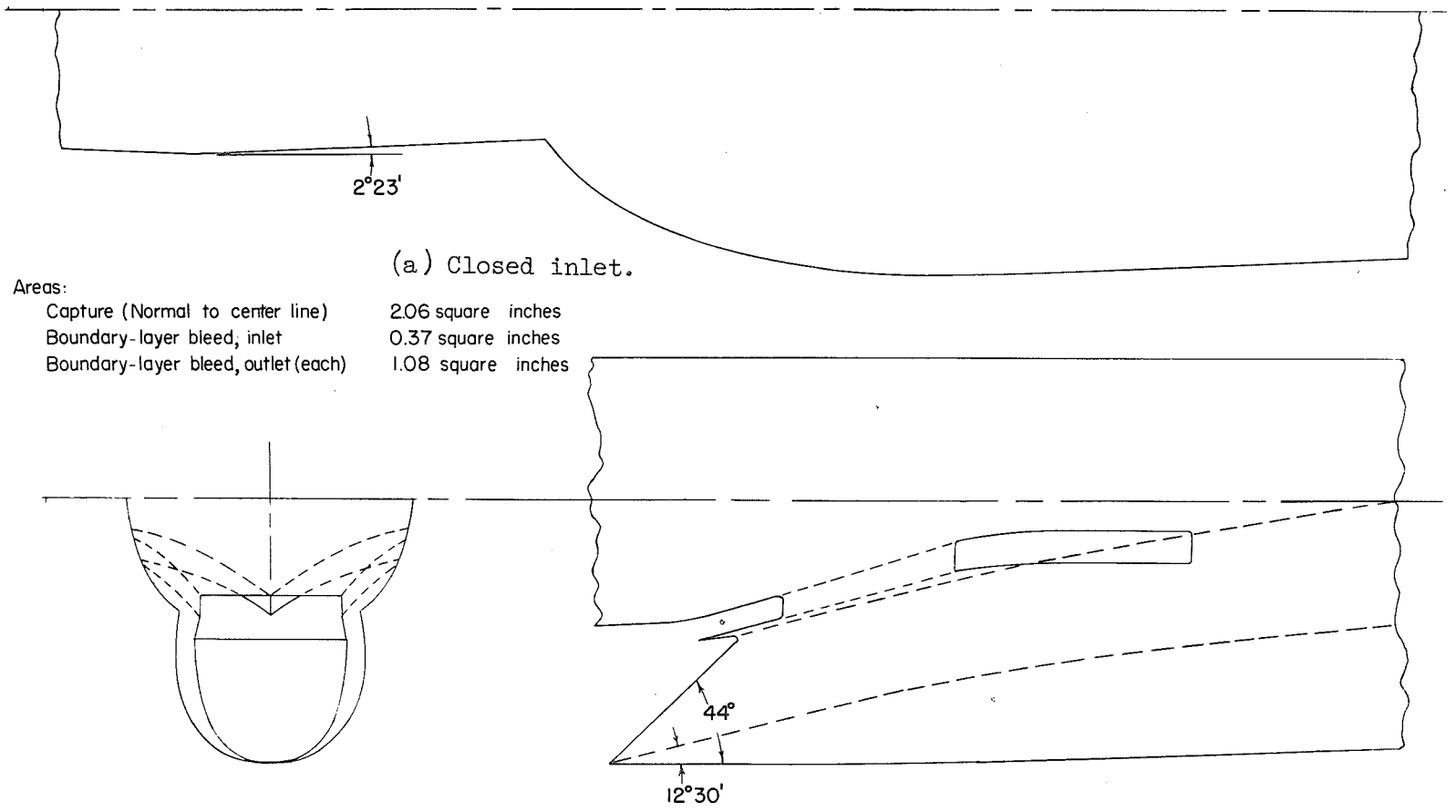

Figure 3.- Inlet details, open and faired closed.

CONFIDENTIAL

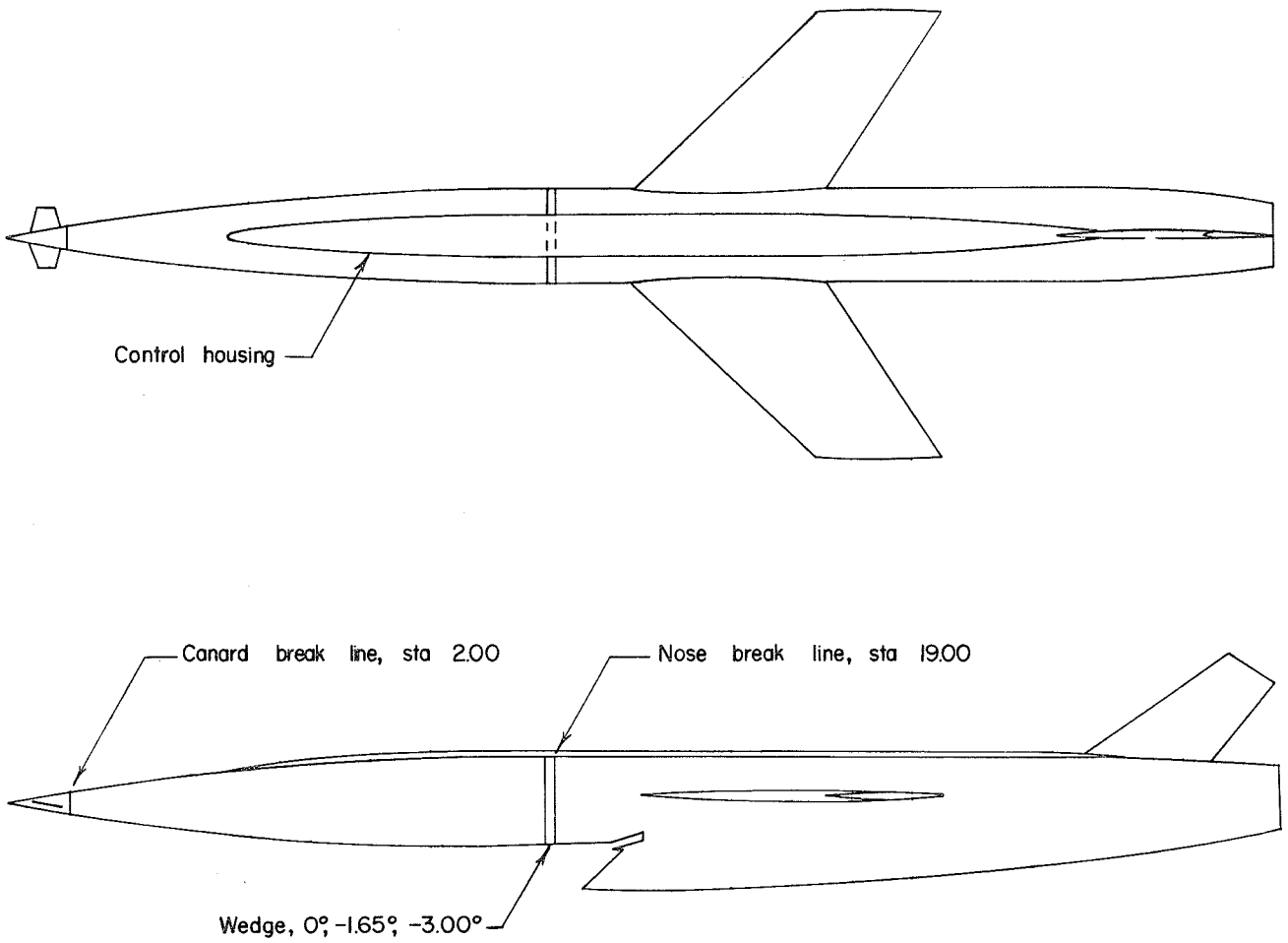

(a) Canard, control housing, and nose wedge.

Figure 4.- Sketches of modifications tested. All dimensions in inches unless otherwise noted. Station 0 is at nose.

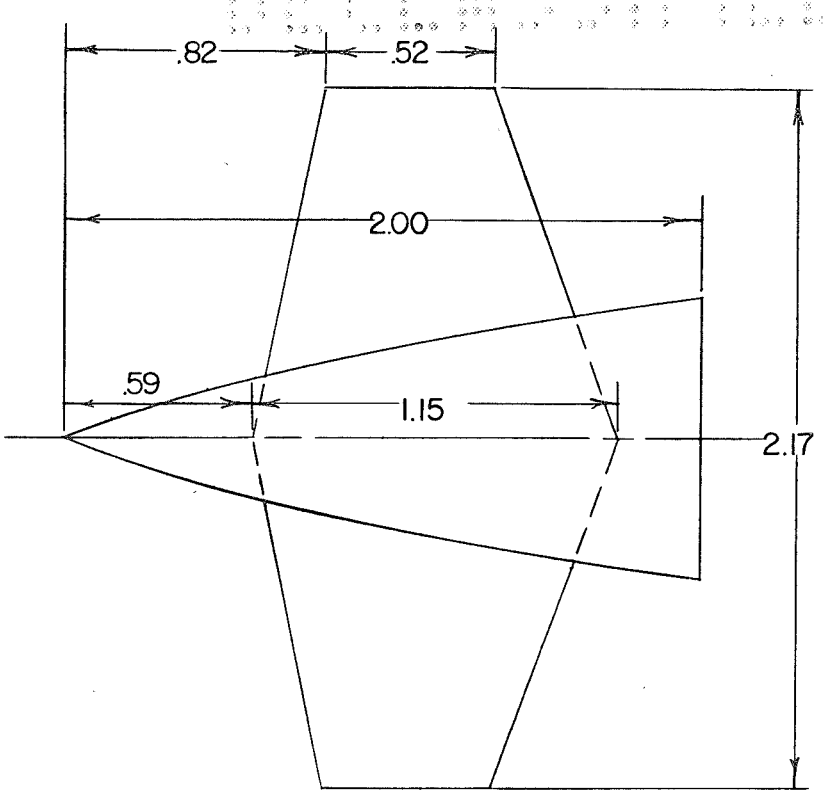

δ=9.5°; exposed area=1.28 sq in.

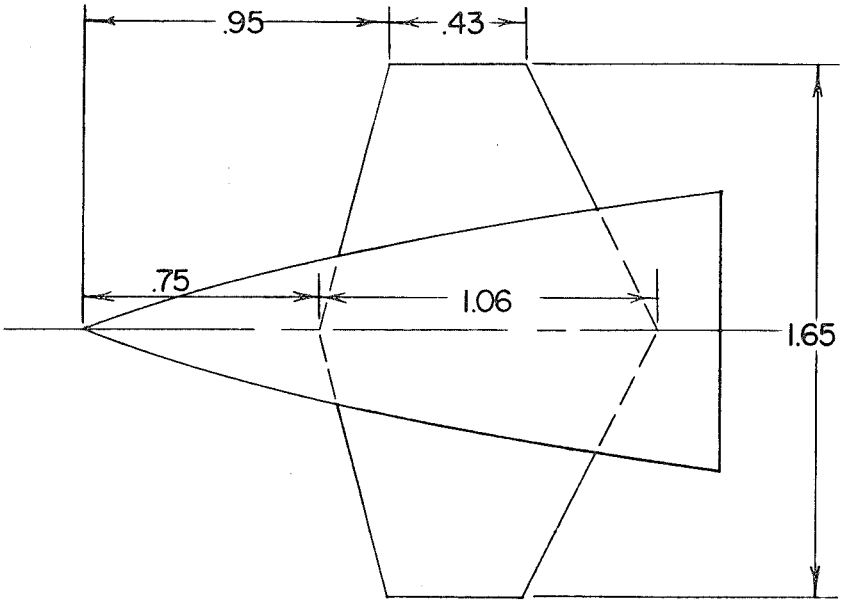

δ=19.1°; exposed area=0.64 sq in.

(b) Details of canards.

Figure 4.- Continued.

CONFIDENTIAL

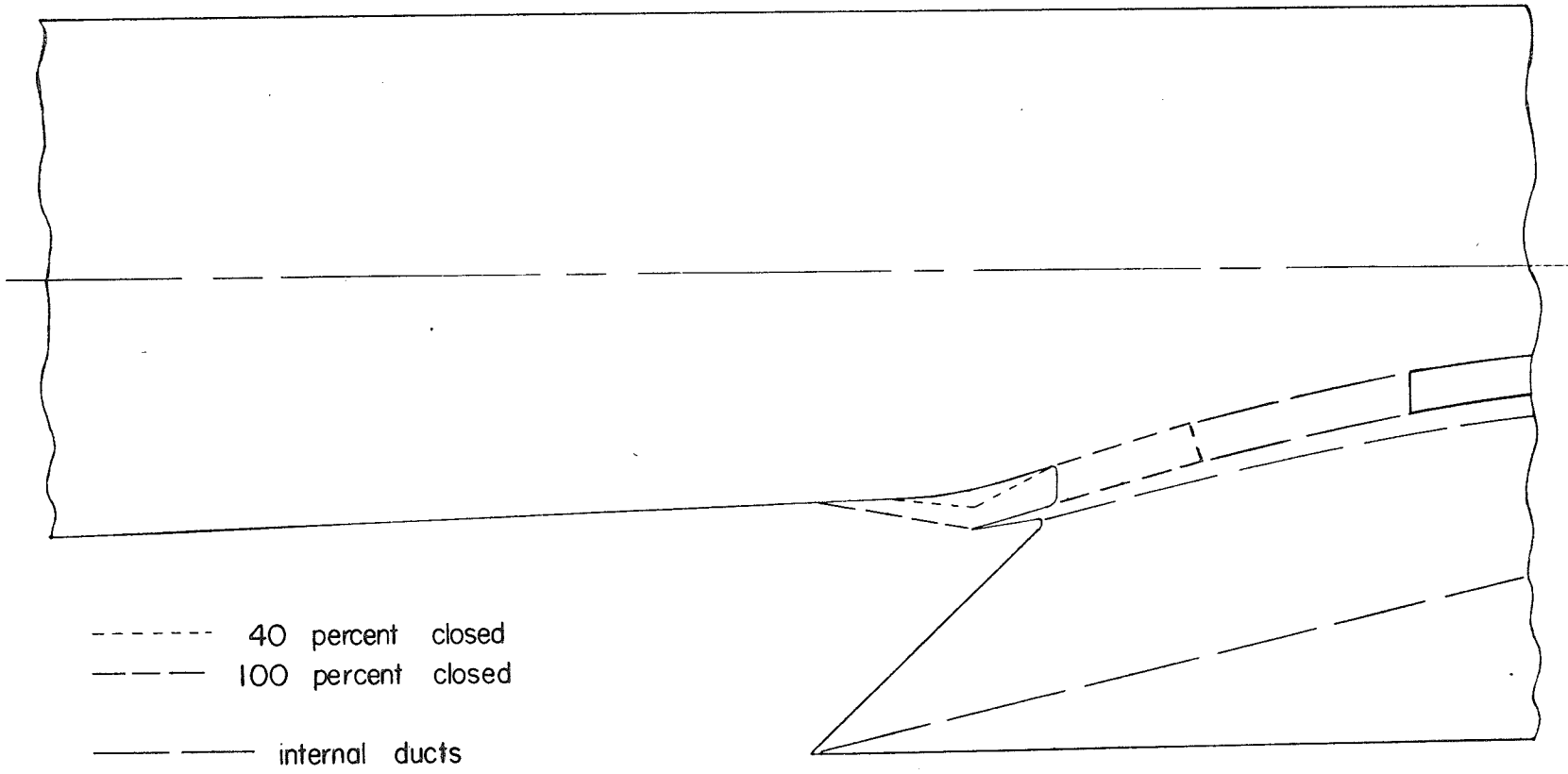

(c) Boundary-layer bleed closures.

Figure 4.- Concluded.

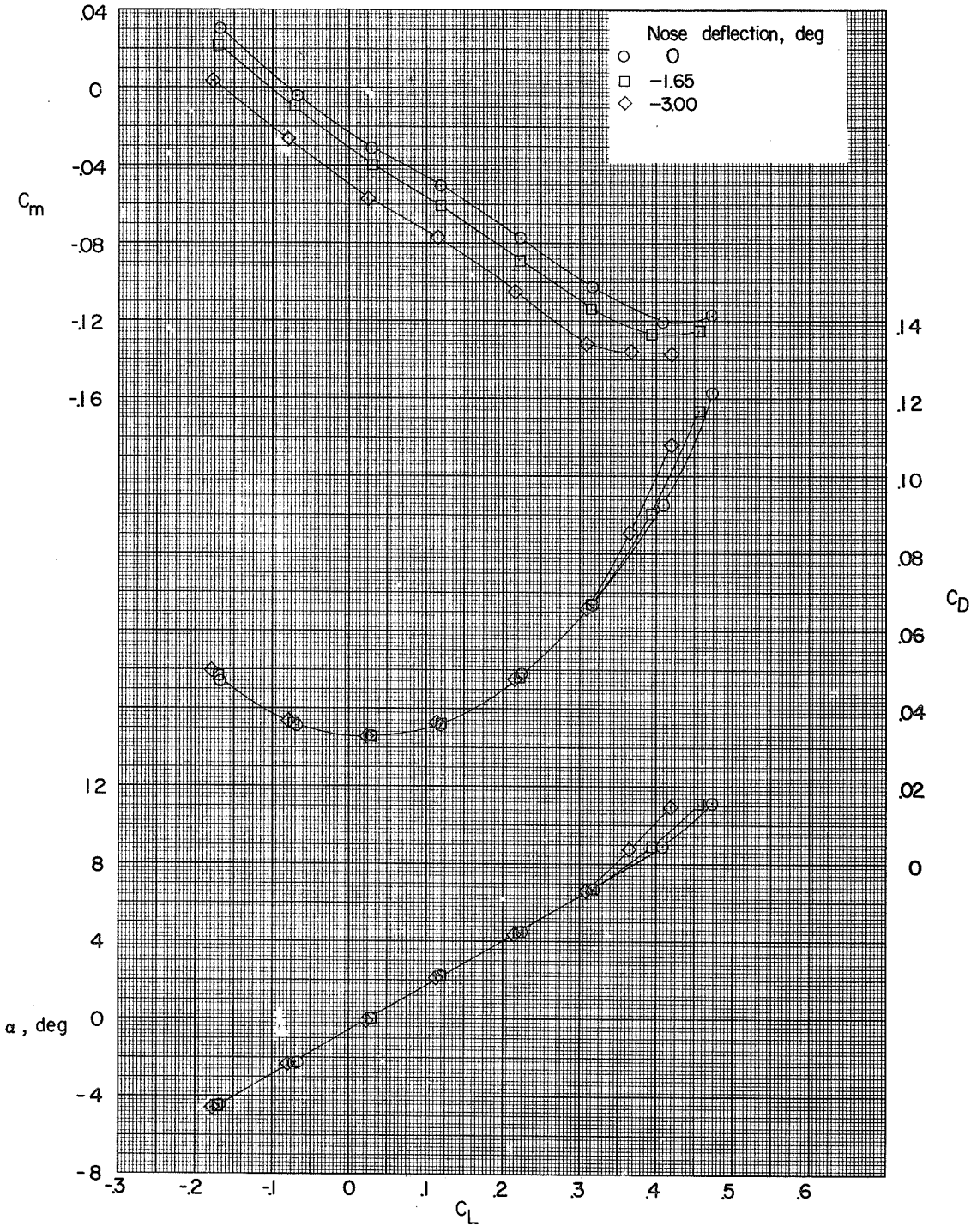

Figure 5.- Effects of nose droop on the aerodynamic characteristics in pitch. $\delta_{e_L} = \delta_{e_R} = 0^o$.

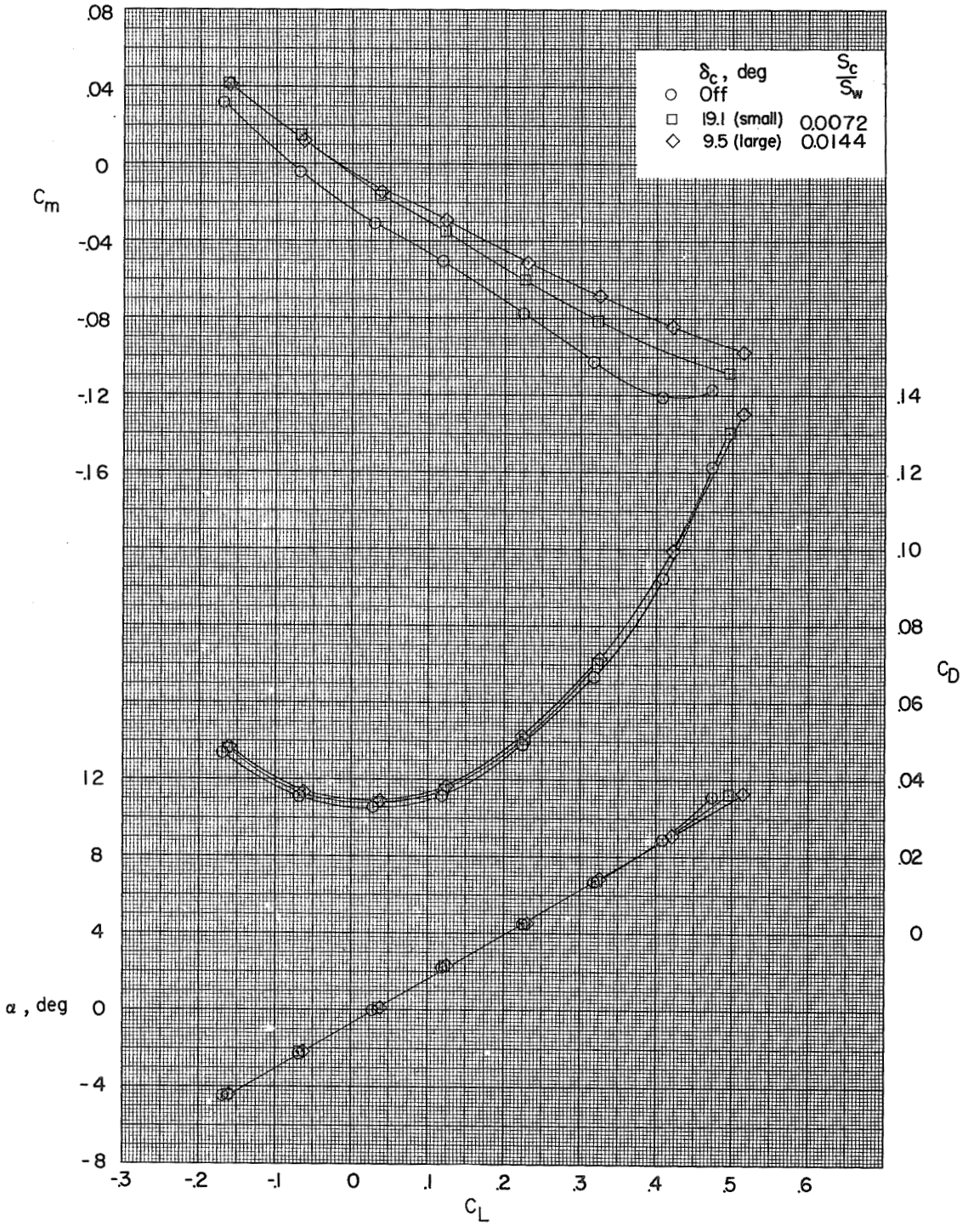

Figure 6.- Effects of canards on the aerodynamic characteristics in pitch. $\delta_{e_L} = \delta_{e_R} = 0^o$.

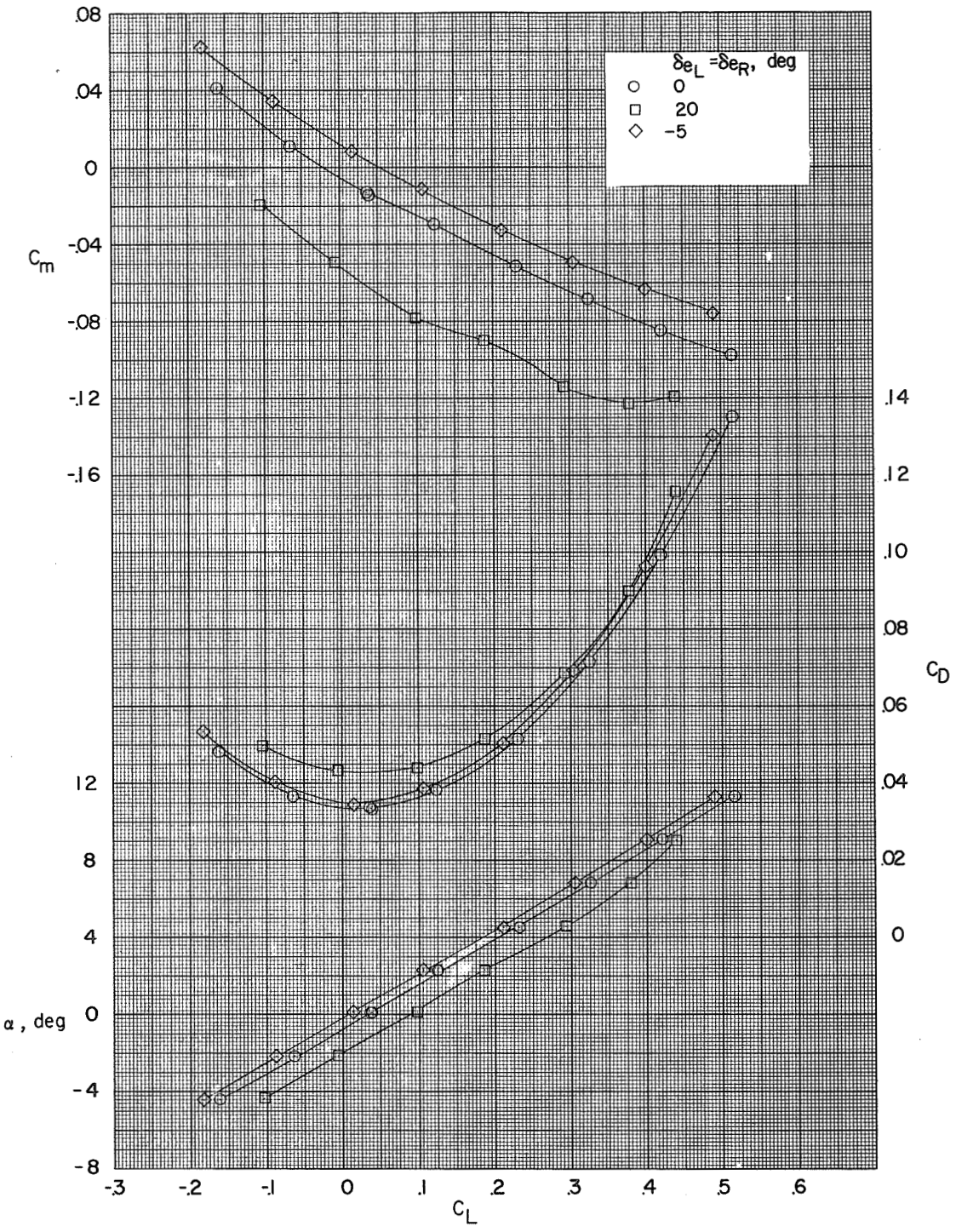

Figure 7.- Effect of elevon deflection on the aerodynamic characteristics in pitch. Large canard, $\delta_c = 9.5^\circ$.

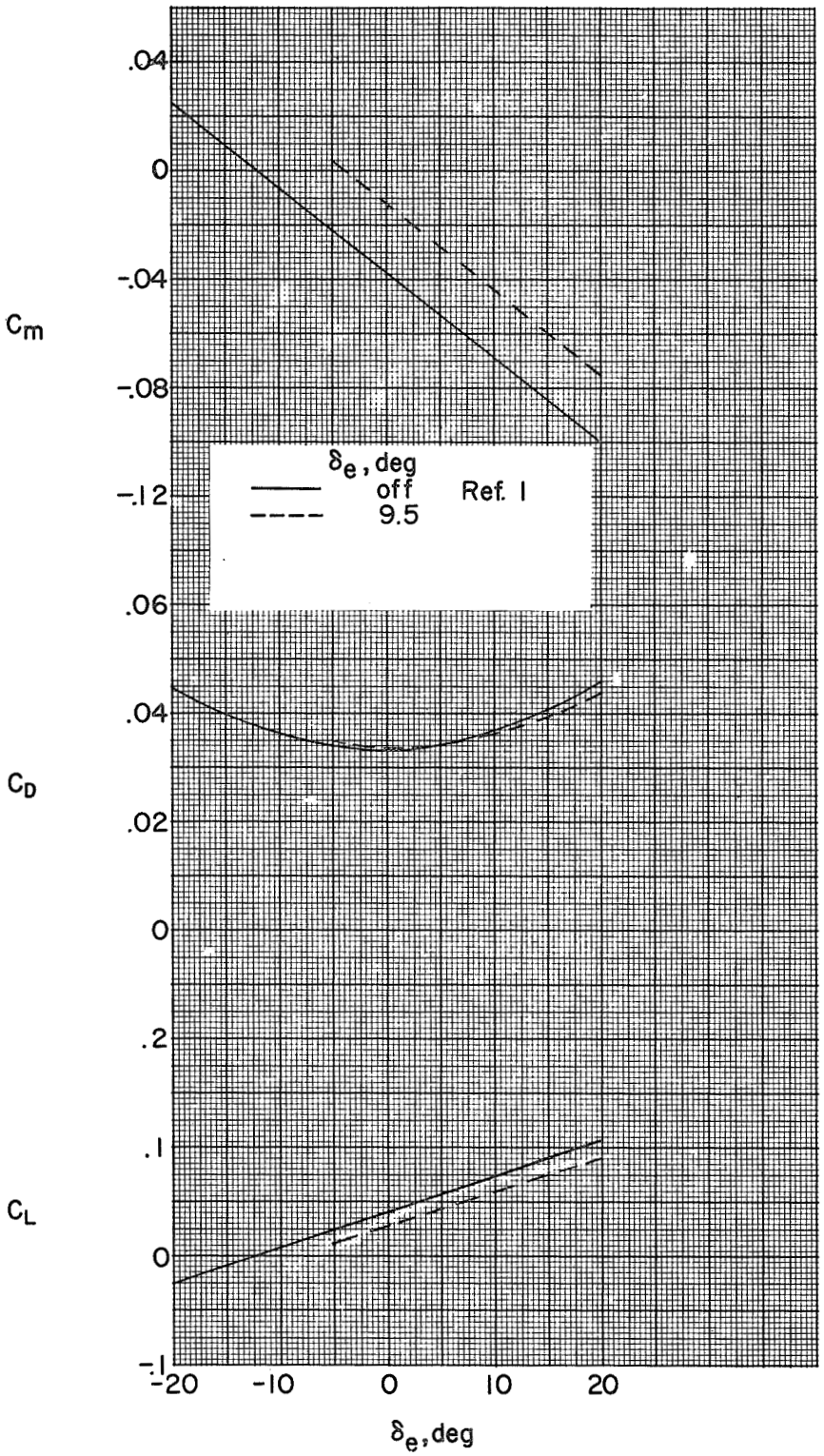

Figure 8.- Effect of the large canard, $\delta_c = 9.5^\circ$, on the variation of lift, drag, and pitching-moment coefficients with elevon deflection. $\alpha = 0^\circ$.

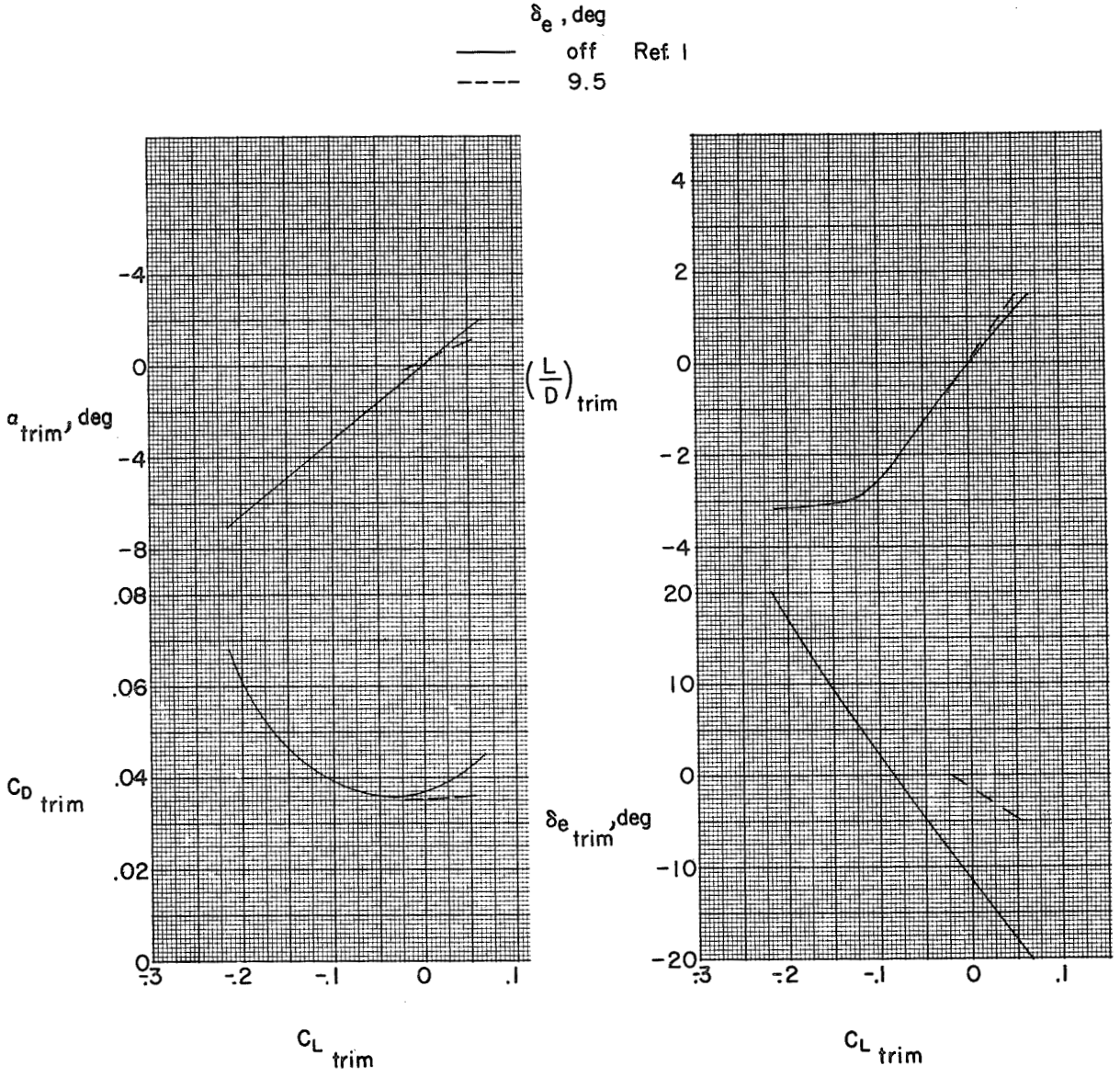

Figure 9.- Effect of the large canard, $\delta_c = 9.5^\circ$, on the longitudinal trim characteristics.

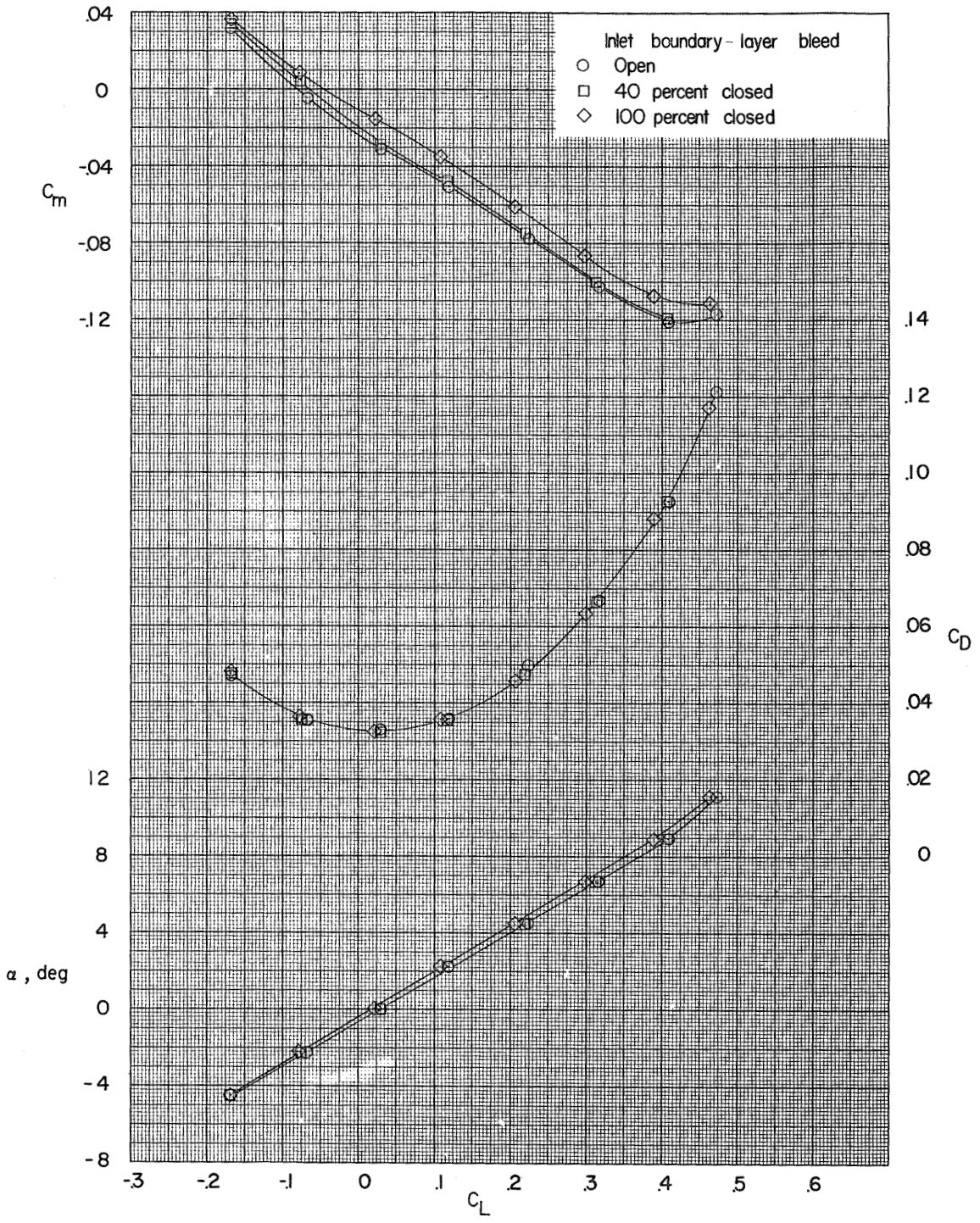

Figure 10.- Effect of varying the amount of boundary-layer bleed closure on the aerodynamic characteristics in pitch. $\delta_{e_L} = \delta_{e_R} = 0^o$; open inlet.

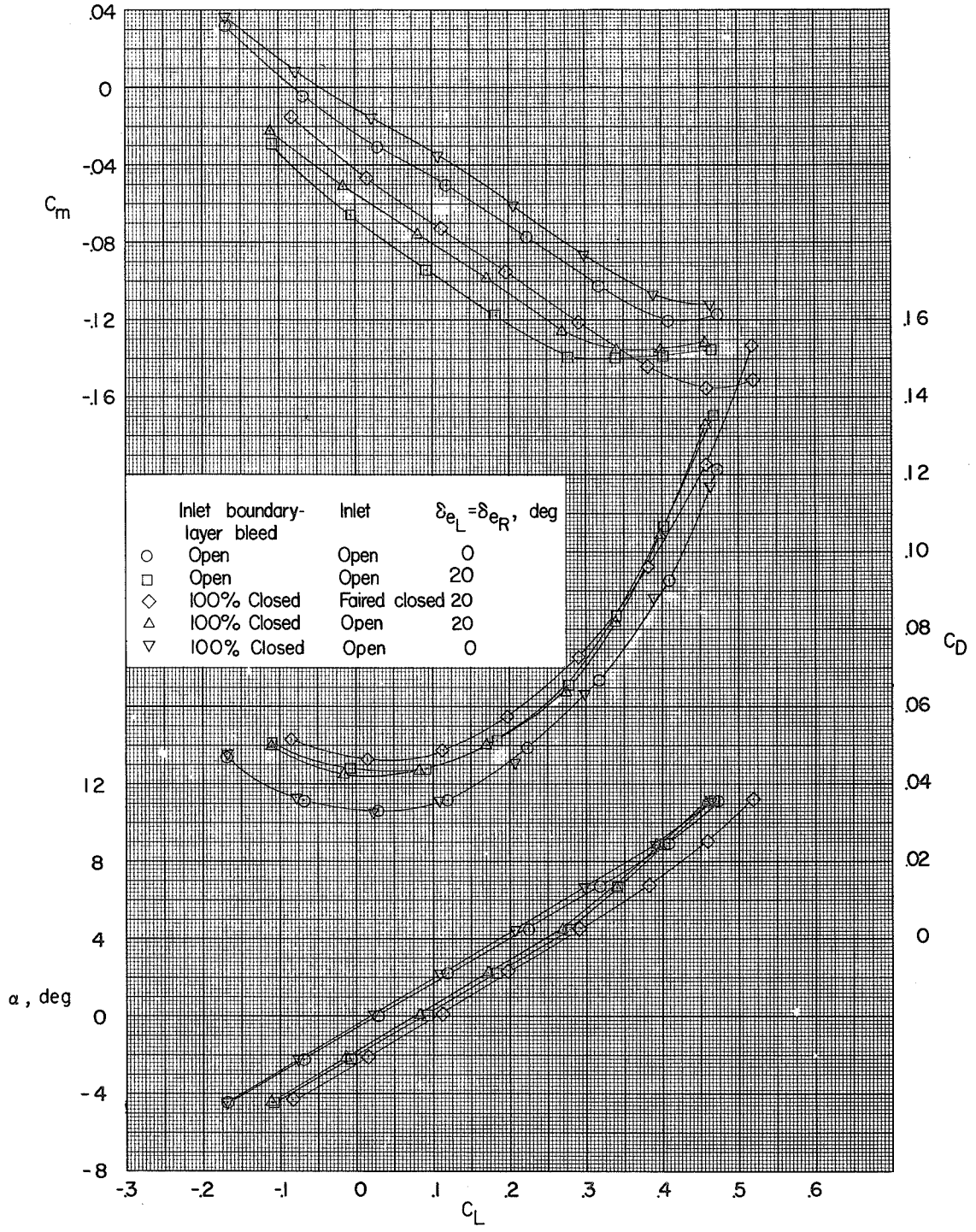

Figure 11.- Effects on the aerodynamic characteristics in pitch of various combinations of boundary-layer closure and open and faired closed inlet for two elevon deflections.

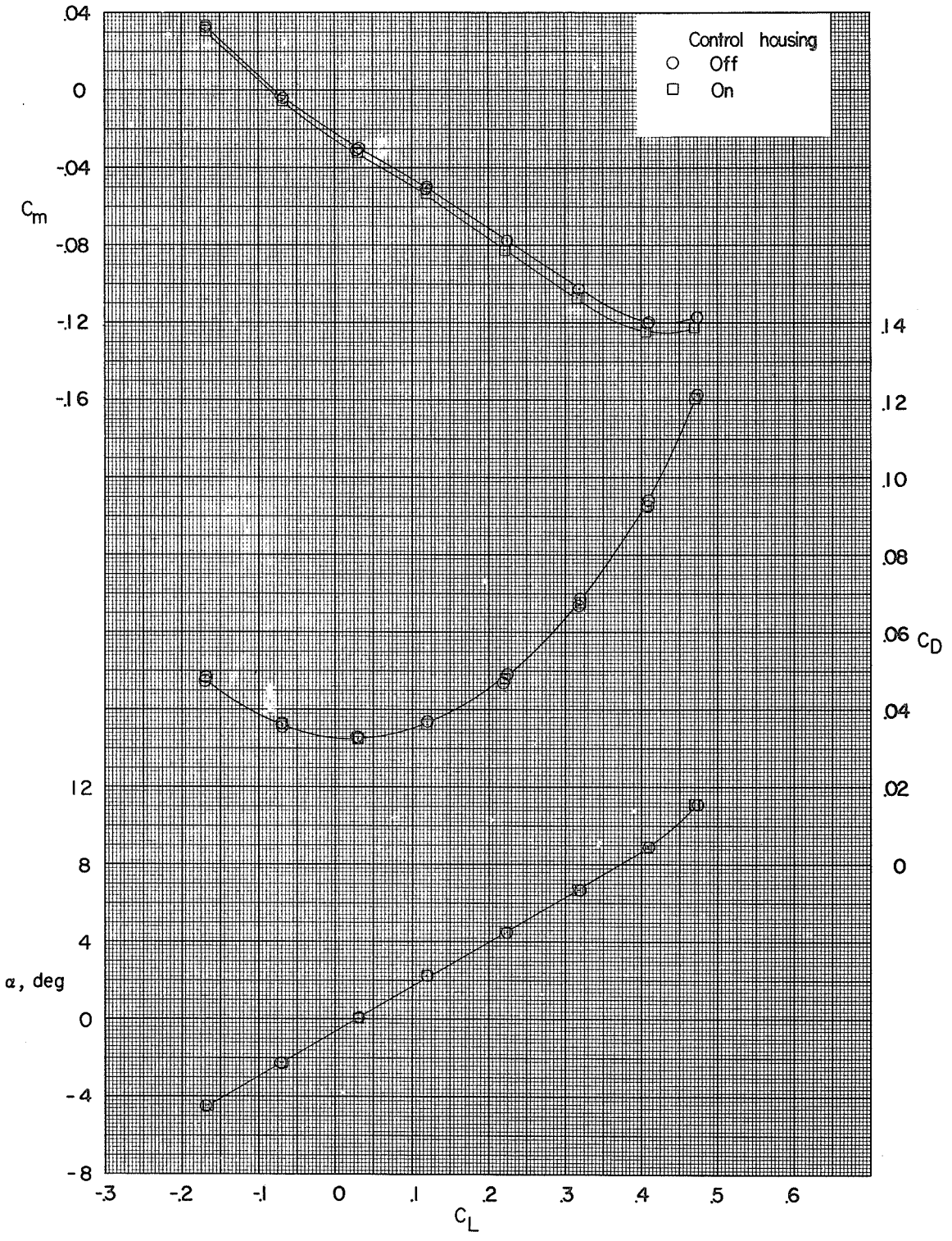

Figure 12.- Effect of control housing on the aerodynamic characteristics in pitch. $\delta_{e_L} = \delta_{e_R} = 0^\circ$.

[redacted]

[redacted]